RSC Advances

ROYAL SOCIETY OF CHEMISTRY

www.rsc.org/advances

ARTICLE Journal Name

Solid state NMR characterization of zeolite Beta based drug formulations containing Ag and sulfadiazine

Received 00th January 20xx,
Accepted 00th January 20xx

DOI: 10.1039/x0xx00000x

www.rsc.org/

Pavletta Shestakova,*[a] Charlotte Martineau,[b] Vesselina Mavrodinova[a] and Margarita Popova[a]

In this study we present a detailed characterization of zeolite Beta-based drug formulations with antibacterial properties, containing Ag and sulfadiazine (SD). Solid state NMR spectroscopy (^{1}H, ^{13}C, ^{29}Si, ^{27}Al and ^{1}H-^{29}Si CP-HETCOR experiments) was applied to address some important questions concerning the changes in zeolite structure as a result of the simultaneous presence of both drugs SD and silver sulfadiazine (AgSD). A mechanism for transformation of octahedral defect framework Al sites and encapsulation of the extraframework Al (EFAl) present in the parent Beta material into framework tetrahedral species as a result of the drug loading procedure is proposed. The analysis of ^{1}H spectra suggested that an ion exchange process between the zeolite protons and Ag ions has occurred upon the solid-state procedure of silver introduction by $AgNO_3$ or AgSD. Suggestions about the location of the drug molecules inside the pores and/or on the crystallite surface are made and the nature of the drug-carrier interactions is discussed. Comparison of ^{1}H spin-lattice (T_1) and spin-spin (T_2) relaxation times of pure drugs and drug loaded formulations indicate amorphization of the drug incorporated into the zeolite pores.

Introduction

The search and development of novel antimicrobial compounds and drug formulations with bactericidal potential is a priority area in pharmaceutical research. Many pathogenic bacteria are able to develop resistance to antibiotics and other antimicrobial drugs commonly used for treatment. During the last decades silver nanoparticles (AgNP) with bactericidal, antifungal, anti-viral and anti-inflammatory properties have been developed and nowadays they are considered to be the new hope in biomedical research.[1-3] In a recent review Mintova et al.[4] have paid a special attention to the preparation of silver loaded nanosized zeolites and their utilization for innovative antimicrobial and medical purposes.

Different approaches have been developed for introduction of silver species in the body including the use of zeolite materials as supports.[5-7] The zeolite materials have many exciting pharmacological potentials, among them one of the most explored being their ability for possible encapsulation and adsorption of different ions and drug molecules in their open framework, and the subsequent delayed release.[8-19]

The nanosized zeolites possess both micropores and textural mesopores able to accommodate different drug molecules. Compared to the mesoporous silica carrier, selective absorption and release of drug molecules with smaller dimensionality can be achieved by choosing an appropriate type of zeolites with proportional pore dimensions. Mostly zeolites Y (diameter of the windows opening 7.4 Å, connected to supercages with 13 Å diameter) and BEA (pore apertures ranging from 6.6 to 7.7 Å) have been examined as supports for drug compounds, which appear to be one of their advanced unconventional applications nowadays.[20] Some authors suggest hypothesis about the mechanism of interaction of different drug molecules with Y type faujasite,[13-15,17-19] its potential for drug loading and kinetics of drug release.[11,17,21] The biological evaluations of these systems containing only drug or silver[6,10,22] or the cytotoxicity of the zeolite nanoparticles itself[23] are also extensively studied. Synergic effects have been demonstrated for combined systems containing silver and antibiotics encapsulated together on non-silica materials as chitosan–silver nanocomposites,[24] or for β-lactam antibiotics combined with silver nanoparticles.[25] Very scarce are, however, the studies on such combined systems based on zeolites as carriers. Laluesa et al.[7] have found strong bactericidal synergy towards S. aureus when paracetic acid was adsorbed in the channels of Ag-ZSM-5. Cerri et al.[26] have applied a successful anti-acne topical therapy with erithromicine supported on natural zeolite clinoptilolite exchanged with Zn-ions.

Synergistic effects of ionic silver with different antibacterials used in the treatment of burn wound infections have been reported more than 20 years ago[27,28] however dual drug systems combining zeolite carriers initially modified with Ag and loaded afterwards with antibiotic have not been examined.

In our previous contribution we have described a new successful and simplified procedure for preparation of dual drug delivery system containing both Ag and sulfadiazine, utilizing zeolite Y as support.[29] The effect of the presence of Ag and the method of the drug introduction on the loading efficiency and the drug release kinetics has been investigated there. Publications in the literature for such a perspective drug delivery system enabling simultaneous controlled release of these two bioactive components are not reported to the best of our knowledge.

The aim of the present study is to give a more detailed characterization of the proposed dual drug formulations expanded to include also nanosized Beta zeolite loaded with SD and AgSD. Investigations on the antimicrobial potential of

[a] Institute of Organic Chemistry with Centre of Phytochemistry, Bulgarian Academy of Sciences, Acad. G. Bonchev str. Bl.9, 1113 Sofia, Bulgaria; e-mail: psd@orgchm.bas.bg
[b] Institut Lavoisier, UMR CNRS 8180, Université de Versailles St. Quentin en Yvelines, Versailles, France.

†Electronic Supplementary Information (ESI) available: deconvoluted ^{27}Al spectrum of HB, ^{13}C CP-MAS spectra, deconvoluted single pulse ^{29}Si spectra of HB and AgB, ^{1}H-^{29}Si CP-HETCOR NMR spectrum of AgSD/HB. See DOI: 10.1039/x0xx00000x

these drug delivery systems have been recently completed and showed promising bactericidal effect on the most frequently applied bacteria strains. The focus of this work is to clarify some important questions that remained unanswered in our previous investigations such as: i) changes in the zeolite structure as a result of the simultaneous presence of Ag, SD or AgSD in the drug formulations, ii) presence of exchange process between the zeolite protons, the Ag ions and the loaded medications, iii) location of the drugs and iv) nature of the drug-carrier interaction depending on the zeolite cations (H^+ or Ag^+). For that purpose we used solid state Magic Angle Spinning (MAS) NMR spectroscopy allowing deeper characterization of the structure and interactions of the studied materials at molecular level. During the last decades solid state NMR has been developed as a powerful and valuable tool for the investigation of structural properties of zeolites and mesoporous[30,31] materials, including their applications as solid supports for drug delivery systems.[32] In addition to structural information the solid state NMR techniques give an insight to the dynamics of the loaded drug molecules as well as to the drug-drug and drug-matrix interactions.[33,34]

Results and Discussion

^{27}Al NMR spectra of the parent (HB) and Ag-modified (AgB) BEA zeolites and their drug-loaded formulations designated as SD/HB, AgSD/HB and SD/AgB are presented in Figure 1. The spectrum of the parent HB material indicates the presence of both framework tetrahedral (signal at 55 ppm) and octahedraly coordinated Al species (signal at 0 ppm). The broad signal observed between 25 ppm and 50 ppm originates from aluminum atoms in pentacoordinated or disturbed tetrahedral coordinated state.[35] Such resonances for protonic Beta zeolite prepared by thermal decomposition of its NH_4^+ form have been observed and reported by other authors.[36,37] Literature data show that, besides the different cationic (oxide/hydroxide) extra-framework Al species (EFAl), also three-coordinated aluminium octahedral entities, coordinating three adsorbed water molecules, are ascertained to be present in zeolite Beta[36,38,39,40] as well as in other types of zeolites such as MCM-22[41] and ZSM-5 zeolite.[42] These species are also known in the literature as framework defect (distorted) sites. NMR studies based on advanced solid state methods such as ^{1}H{^{27}Al} spin-echo double resonance MAS NMR and {^{1}H}-^{27}Al CP-MAS NMR[43] and more recently ^{27}Al 3QMAS and DQMAS experiments demonstrated that the signal at around 0 ppm in the ^{27}Al NMR spectrum has complex substructure and originates from at least two types of *octahedrally* coordinated aluminum atoms: the six-coordinated EFAl species [$Al(OH)_3.3H_2O$ at around -0.6 ppm] and the defect framework octahedral sites representing three-coordinate framework Al species with three adsorbed water molecules (at around -0.1 ppm).[44,45] It is well known that when protons are compensating the negative charge of zeolite beta, severe disturbance in the coordination of some framework aluminium atoms occurs and lattice defects are generated. In the presence of water the distorted sites as the tri-coordinated framework entities may also feature an octahedral symmetry or undergo hydrolysis of the Al-O bonds.[38]

Loading of the parent HB zeolite with SD as well as the introduction of Ag^+ ions by $AgNO_3$ or AgSD result in disappearance or dramatic decrease of the ^{27}Al signal at around 0 ppm, assigned to both ~~originating from~~ the extra-lattice cationic species (EFAl) and the three-coordinated framework Al (Figure 1). Embedding of SD into the Ag-modified sample (AgB) does not lead to significant changes in its ^{27}Al NMR spectrum. This result implies that the Al atoms which have already restored their tetrahedral positions by silver introduction do not change their coordination upon SD loading and still remain inserted and stabilized in the lattice.

It is well known, that restoration (healing) of the framework disruption accompanied by disappearance of the resonance at 0 ppm can be attained when charge compensating cations such as Na^+, K^+ or extralattice cationic Al species generated by high temperature hydrothermal treatment are introduced[37,46,47] or back ammonation is applied to the calcined H-form of zeolite Beta.[36,46,48] Thus, the observed disappearance of the signal at 0 ppm in the ^{27}Al spectrum of our silver modified or AgSD loaded parent HB zeolite (Figure 1, samples AgB and AgSD/HB), proves the introduction of silver in cationic positions by the applied SSIE procedure.

The octahedral–tetrahedral framework aluminum transformations in zeolite B in presence of ammonia were first suggested by Bourgeat-Lami et al.[36] and further investigated in more details with advanced solid state NMR methods by other authors.[38,43] These authors showed that the octahedral Al species that undergo transformation to tetrahedral sites are mainly the three-coordinated framework defect species in the

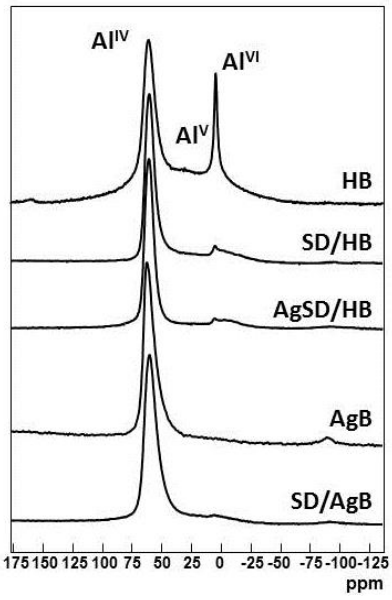

Figure 1. ^{27}Al MAS NMR spectra of the studied samples. The resonances are assigned to the various Al coordination environments.

vicinity of silanol groups generated as a result of breaking of framework Si-O-Al bridges. Thus the proposed mechanism of reintegration of the defect framework Al sites into the zeolite lattice ~~reinsertion of the EFAl~~ in the presence of Ag cations, originating either from $AgNO_3$ or from AgSD is presented in Scheme 1, panels A and B respectively. An alternative mechanism involving also the conversion of the octahedral six-coordinated EFAl species to tetrahedral framework sites previously suggested by Hunger et. al.[38] is given in Scheme S1 (ESI). The two mechanisms could operate simultaneously in the presence of Ag^+, SD and AgSD, resulting in disappearance of the signal at 0 ppm in the ^{27}Al spectrum.

An effect of healing the framework defects and restoration of Al in tetrahedral framework positions is clearly visible also when sulfadiazine is introduced by the solid-state milling procedure of SD with the H-form of the zeolite (Figure 1, sample SD/HB). As a result of the drug adsorption, disappearance of the ^{27}Al NMR signal at 0 ppm is observed for this formulation as well. Analogous effect of strong decrease of the ^{27}Al NMR signal at 0 ppm characteristic for the octahedral Al in several HY carriers loaded with aspirin[19] or 5-fluorouracil[18] has been reported by S. Larsen *et al*. The authors attribute this effect to the formation of strongly bound complexes of the drug with the aluminum extraframework sites. Interestingly, no such effect of disappearance of this signal is detected by Horcajada *et al.* for ibuprofen-loaded dealuminated Y zeolite.[17] In this case the authors do not observe any substantial changes in the 0 ppm resonance of the ~~extraframework~~ octahedral Al and do not discuss the changes in the intensity of both lattice and octahedral ^{27}Al NMR signals of the zeolite carriers before and after drug loading. They proposed different nature of interaction of ibuprofen with the carrier depending on the amount of extra-lattice Al based on the FT-IR results.

Our suggestion explaining the observed disappearance of the 0 ppm signal for SD loaded HB zeolite is that a proton from a silanol group, adjacent to the tri-coordinated, defect Al atom shifts to the sulfonamide NH group of the sulfadiazine molecule forming quaternary $-(NH_2^+)-$ group as cationic species (Scheme 1 and Scheme S1, panel C). These species act in a similar way as the well-known "healing cation agents" like NH_4^+, Na^+, etc. and restore the tetrahedral coordination of the neighbor Al atoms. We suggest that the proton from the $-(NH_2^+)-$quaternary group of the protonated SD, is highly mobile and exchanges between the zeolite lattice and the drug molecule, resulting in fast dynamic equilibrium between the protonated and non-protonated form of SD. The lack of chemical shift changes in the ^{13}C CP-MAS NMR spectrum of SD/HB compared to the ^{13}C CP-MAS spectrum of the pure SD (Figure S2, ESI) supports this assumption.

Additional indication for such an exchange came from the ^1H NMR spectra of the preparations presented in Figure 2. The ^1H spectrum of SD/HB material shows that the signal at around 10 ppm characteristic for the NH group of SD is broader and has lower relative intensity as compared to the NH signal in the spectrum of the pure SD. This NH signal broadening is usually associated with the existence of dynamic process

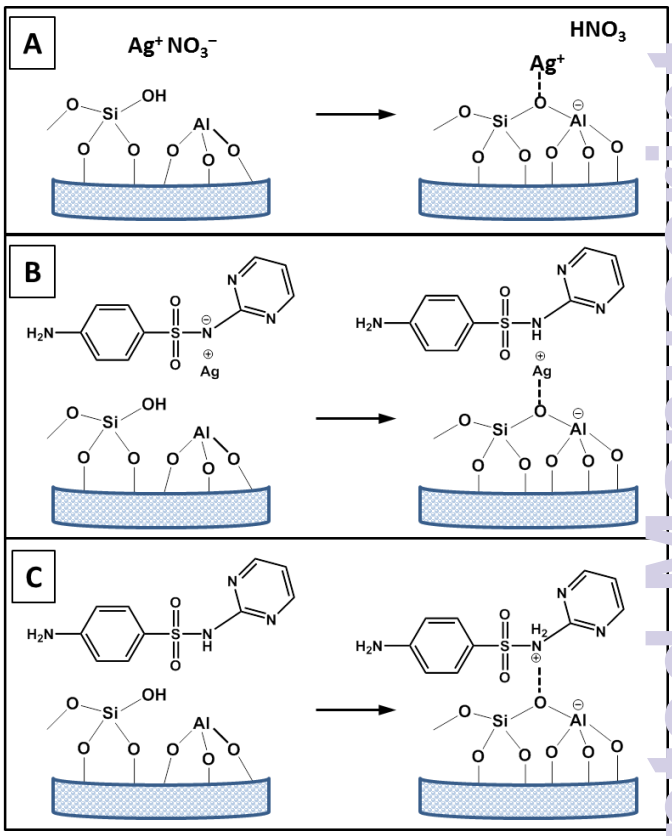

Scheme 1. Mechanism of reintegration of the defect framework Al sites into the zeolite framework in the presence of Ag^+ (A, B) and SD (C).

involving an exchange of the NH proton between two sites. In addition, comparison of the ^1H spectra of SD/HB and SD/AgB shows higher NH signal intensity in the latter. Indeed it is expected that in the case of SD/AgB the exchange process will be less pronounced since the charge-compensating positive Ag^+ species are less mobile.

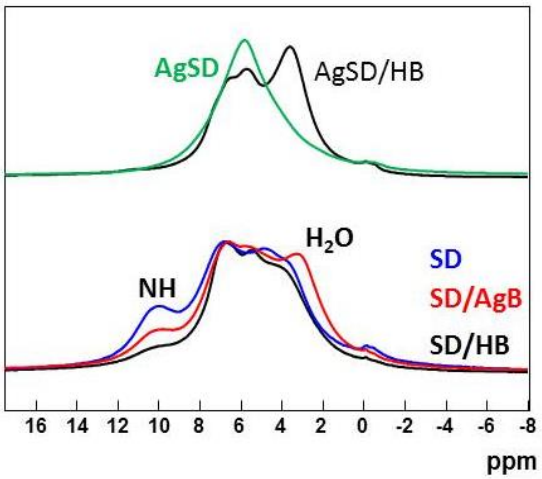

Figure 2. ^1H MAS NMR spectra of samples SD/HB, SD/AgB and AgSD/HB. For comparison the ^1H MAS NMR spectra of the pure SD and AgSD compounds are displayed.

To give further evidence for the suggested mechanism including the involvement of the silanol groups originating ether from the opening of the SiOHAl bridges or from the framework silanol groups in the vicinity of the framework defect Al sites we measured ^{1}H spectra of the studied materials. The ^{1}H spectra of the samples dried overnight at 100 °C to remove the strong water signal, demonstrate that the signals within the region of 0-2 ppm corresponding to the Al(OH) from EFAl and defect FAl moieties, and silanol (SiOH) protons have lower intensity or almost disappear in the spectra of the drug loaded samples AgB, SD/HB, SD/AgB and AgSD/HB (Figure S3, ESI). Unfortunately detailed analysis of the ^{1}H spectra of the drug loaded samples in the region of the bridging SiOHAl groups (from 3.8 to 5 ppm) is hampered by the overlap with the strong signal from the SD aromatic protons which dominates the ^{1}H spectra.

The structural transformations in the zeolite materials as a result of Ag^{+} cation loading could be also followed by ^{29}Si NMR spectroscopy (Figure 3, left). The five different structural environments of the tetrahedrally coordinated Si atoms, denoted as Si(nAl), where n = 0, 1, 2, 3 and 4, have characteristic chemical shifts in the ^{29}Si NMR spectra, while the relative intensities of the signals for the different Si(nAl) species reflect the composition of the zeolite framework. The single pulse ^{29}Si NMR spectra of the different materials are almost identical (Figure 3, left) and show two partially overlapping signals. The signal at -110 ppm is characteristic for Si(0Al) species, while the second signal at -103 ppm indicates the presence of Si(1Al) and Si(1OH) species. The single pulse ^{29}Si spectra reveal that there is a little difference in framework structure and composition as a result of cation exchange or drug loading. This result is not surprising considering the mechanism of cation (drug) induced octahedral to tetrahedral Al transformations as presented in Scheme 1. During this process the silanol groups from the defect sites of the parent zeolite (Si(1OH) species), are transformed into framework Brønsted centers (corresponding to Si(1Al)), which give a signal within the same chemical shift range in the ^{29}Si spectrum. Thus the loss of signal due to silanol groups is compensated by formation of Brønsted sites by the restoration of the Al in framework positions and the total intensity of the signal at around -103 ppm in the ^{29}Si spectra resulting from both Si(1OH) and Si(1Al) species is therefore not significantly affected by the reinsertion of the octahedral ~~EF~~Al species in to the zeolite framework. For example by deconvolution of ^{29}Si spectra of samples HB and AgB it was estimated that the total amount of the [Si(1OH) + Si(1Al)] species has increased by around 13% upon drug loading in AgB as compared to the parent material HB. (Figure S4, ESI).

Indications for the drug-matrix interactions and the localization of the drug within the zeolite carrier have been obtained by ^{29}Si and ^{13}C CP MAS spectra. The cross polarization (CP) technique is based on transfer of polarization from abundant spins (^{1}H) to low sensitivity nuclei (^{29}Si or ^{13}C) via through space dipole-dipolar interactions. Thus this method allows to selectively enhancing the signals from ^{29}Si and ^{13}C sites that have ^{1}H nuclei in their vicinity, originating either from OH groups or SD molecules. In addition, it is expected that if the drug molecules bind covalently to the zeolite matrix this will result in change of the chemical shifts of the drug. The ^{13}C CP MAS spectra of the drug loaded samples (Figure S2) show that there is no change in the signal linewidth and in the chemical shifts of the supported drug molecules as compared to the pure drug. This implies that the loaded drug is not chemically bound neither to the H- or Ag-form of the support.

Figure 3 (right) shows the ^{1}H → ^{29}Si CP MAS spectra of the studied materials. In the ^{29}Si CP MAS spectrum of the parent zeolite (Figure 3, spectrum of HB) the signal for Q_3 sites is enhanced due to the presence of the adjacent OH groups in the Si(1OH) species, while the signal for Si(0Al) species has much lower intensity due to the lack of neighboring silanols. Similar spectral pattern is observed in the spectrum of AgB material (Figure 3, right), however, the relative Q_3 signal intensity is slightly lower, as compared to the Q_3 signal intensity in the parent zeolite, due to the transformation of some Si(1OH) species into Si(1Al) species as a result of the reinsertion of the octahedral ~~EF~~Al species into the zeolite matrix. The spectra of the three drug loaded samples show

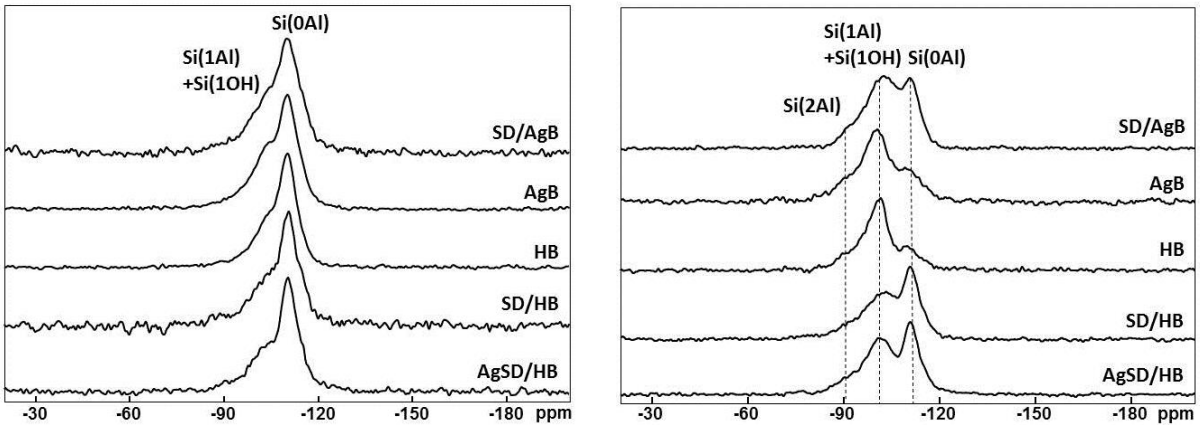

Figure 3. Single pulse ^{29}Si MAS NMR (left) and ^{1}H→^{29}Si CPMAS (right) NMR spectra of the studied samples. The ^{29}Si resonances are assigned to the various Q_n species in the zeolite.

enhancement of the Si(0Al) signal as compared to its intensity in the parent material (Figure 3, right, samples SD/HB, SD/AgB and AgSD/HB). This result implies that the loaded drug is predominantly localized in the vicinity of Si(0Al) species and a large amount of the drug is most probably included within the zeolite pores. This is particularly valid for samples SD/HB and AgSD/HB, where the intensity of the Q_4 signal (Si(0Al) species) is higher as compared to Q_3 resonance intensity. For SD/AgB, where SD is loaded into Ag modified zeolite, the two signals have similar intensities, which suggests that part of the drug is incorporated also within the zeolite channels. This finding could be explained if we assume that in the Ag modified material the zeolite pores are already partially occupied by Ag during the solid-state ion exchange process which makes them less accessible to the drug molecules and hampers the incorporation of the drug within the pores.

^{1}H spectra of samples SD/HB, SD/AgB and pure SD, measured after dehydration of the samples at 100 °C for one night, were used to quantify the relative amount of the drug distributed within and outside the pores (Figure 4). The spectra show that the NH signal intensity of SD is lower when the drug is loaded into non-modified HB zeolite as compared to the Ag-modified carrier. We suggest that when the drug molecules are confined within the pores, the NH-protons from SD are in a fast exchange with zeolite protons and therefore they are not detected in the zeolite ^{1}H spectrum. In contrast the NH protons from SD molecules outside the pores are not involved in exchange, and hence the signal is visible in the ^{1}H spectrum. By assuming the NH intensity of pure SD as 100% (outside the pores) we calculated that for SD/AgB the amount of the drug outside the pores is 58%, while for SD/HB sample it is 40%.

Further evidence for the partitioning of the SD within and outside the zeolite pores is provided by the ^{13}C CP MAS spectrum of SD/AgB material. For this sample all ^{13}C resonances are slightly broader as compared to the signals in both the ^{13}C spectra of the SD loaded non-modified carrier and of the pure drug (Figure S2, spectra of SD/AgB, SD/HB and SD, ESI). This noticeable anisotropic broadening could be explained with the distribution of the drug between the two environments.

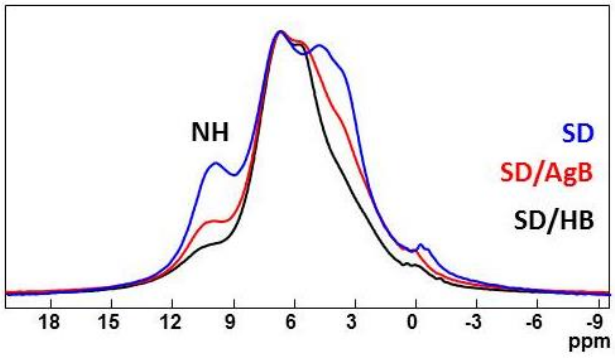

Figure 4. ^{1}H MAS (30 kHz) NMR spectra of SD/HB, SD/AgB and pure SD, measured after heating the samples at 100 °C for one night.

A more detailed insight into the incorporation of the drug within the zeolite matrix is given by the 2D ^{1}H-^{29}Si HETCOR spectrum (Figure 5). This experiment exploits the dipolar interactions between ^{1}H and ^{29}Si nuclei and gives information about the through space proximity between the respective structural fragments. Figure 5 shows the ^{1}H-^{29}Si HETCOR spectrum of sample SD/AgB. The strong correlation peak detected between the Si(0Al) sites and SD aromatic and NH protons evidences the localization of the drug near the Q_4 structures. Another correlation peak, however of lower intensity, is also observed between the aromatic protons of SD and the signal at -103 ppm corresponding to [Si(1OH) + Si(1Al)] sites. Similar result was obtained from the 2D ^{1}H-^{29}Si HETCOR spectrum of AgSD/HB samples (Figure S5, ESI), indicating the identical behavior of the two drug loaded samples SD/AgB and AgSD/HB.

^{1}H spin-lattice (T_1) and spin-spin (T_2) relaxation times give additional insight into the structure and dynamics of the adsorbed drug (Table 1). The results show that T_1 relaxation times of the loaded drug molecules are much shorter (4 s) in all drug formulations as compared with the T_1 values of the pure drugs (30 s for SD and 50 s for AgSD). These results indicate that the drug molecules incorporated into the zeolite matrix are no longer in crystalline form. Such amorphisation of the drug upon inclusion into the zeolite carrier is in agreement with our previous XRD data.[29] The analysis of T_2 relaxation curves shows that the relaxation data for the pure drugs (SD and AgSD) were well fitted with mono-exponential decay giving similar relaxation times of 0.14 ms and 0.11 ms for SD and AgSD respectively, while the T_2 data of the zeolite loaded drugs were best fitted with two-exponential function. The results show that there is no significant difference between the T_2 values for the three drug loaded samples. The T_2 results for the drug loaded zeolites indicate the presence of one fast relaxing component with T_2 value similar to the T_2 of the pure drugs and a second slow relaxing component with much longer T_2. The first component was assigned to the drug outside the zeolite pores which is less mobile being in a crystalline phase.

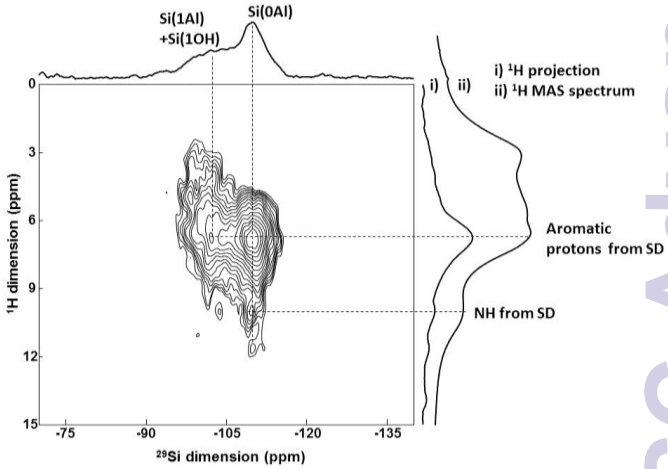

Figure 5. ^{1}H-^{29}Si CP-HETCOR NMR correlation spectrum of SD/AgB.

Table 1. T_1 and T_2 relaxation times of SD and AgSD in pure samples and in drug loaded BEA materials.

Sample	T_1 (s)	T_2[a] (ms)	
SD	30	0.14	
AgSD	50	0.11	
SD/HB	4	0.10 (0.52)	0.58 (0.48)
SD/AgB	4	0.10 (0.57)	0.53 (0.43)
AgSD/HB	4	0.12 (0.57)	0.67 (0.43)

[a]Data in parenthesis represent the molar fractions of the T_2 components.

The component with longer T_2 was assigned to the drug incorporated in the pores which is in an amorphous state and thus more mobile (hence longer T_2). The quantitative assessment of the two components assigned to the drug outside and within the pores indicates that the drug is almost equally partitioned between the two environments, with a slight excess of the drug outside the zeolite pores for SD/AgB sample as compared to the SD/HB sample. These results are in agreement with the conclusions drawn on the basis of T_1 relaxation times analysis and follow the general trend of the data obtained from the ^{1}H spectra (Figure 4).

Experimental

Materials

Zeolite beta nanoparticles were synthesized according to Ref. [49]. The synthesis procedure includes the preparation of a precursor mixture with the following molar composition: Al2O3 = 0.25, R = 9.0, Na2O = 0.35, SiO2 = 25.0, H2O = 295.0, where R is the organic template agent tetramethylammonium (TEA) (Sigma, 20% TEAOH in water). The silica source was derived from a colloidal silica suspension Bindzil 30/360 (Eka Nobel, Sweden) containing 31.1 wt% SiO2 and 0.6 wt% Na2O. The suspension was freeze-dried to powder. The aluminum source was aluminum isopropylate (Sigma). The obtained initial mixture was subjected to hydrothermal treatment at 100°C for 9 days. The crystalline nanoparticles were purified by three times centrifugation at 20,000 rpm for 1 h, followed by re-dispersion in distilled water using an ultrasonic bath to obtain a colloidal sol with a pH of about 9.5. The as-synthesized zeolite was dried at 120°C. The template was removed by calcinations in N2 (at two steps, at 450oC and then at 520oC) followed by final air heating at 520oC, in a tubular furnace in a shallow bath, for 6 hours totally, so as H-form designated as HB to be obtained (Table 2).

Host-guest system preparation. Silver and sulfadiazine loading

Ag-exchanged BEA zeolite is prepared by the solid-state ion exchange (SSIE) technique described in our previous contribution,[29] viz. by milling $AgNO_3$+HB(FD) mixture in a vibrational ball mill for 3 min and heating it for 2h at 520°C in air. The molar ratio Ag to Al was 1. The resulting powder was designated as AgB. The textural characteristics of the parent (HB) and Ag modified (AgB) BEA materials are given in Table 2.

The deposition of the sulfadiazine drug was made at room temperature by high-energy milling of sulfadiazine and HB or AgB modification in a vibrational ball mill at 0.8:1 sulfadiazine to zeolite weight ratio. The resulting preparations were designated as SD/HB and SD/AgB respectively.

Loading of silver sulfadiazine drug (AgSD) was performed by mixing of HB zeolite with appropriate amount of AgSD so as to ensure the same amount of introduced silver as in case of AgB sample. After adding of the drug to the zeolite the mixture was stirred in a vibrational ball mill for 30 min at room temperature and then heated up to 80°C (3°C/min) in N_2 flow and left at this temperature for 30 min.

Methods

The solid-state MAS NMR spectra were recorded on an Avance 500 Bruker NMR spectrometer (static magnetic field B_0 = 11.7 T, corresponding to Larmor frequencies of 500.3, 130.3, 125.7 and 99.0 MHz for ^{1}H, ^{27}Al, ^{13}C and ^{29}Si, respectively). The samples were packed in either 2.5 mm or 3.2 mm outer diameter zirconia rotors and spun at 10 to 30 kHz MAS rate depending on the experiment.

The ^{1}H NMR spectra were recorded at 30 kHz using a Hahn-echo pulse sequence, with 2.5 μs 90° pulse length and an inter-pulse delay synchronized with one rotor period. Typically 16 transients were accumulated for each sample with 2 s recycle delay. The ^{1}H→^{13}C cross-polarization (CPMAS) NMR spectra were recorded at MAS 10 kHz, using a 3 μs 90° pulse for ^{1}H. The contact time was set to 3 ms. The radio-frequency (RF) field on ^{13}C was set to 50 kHz and the ^{1}H RF field was adjusted to meet the n = +1 Hartmann-Hahn condition. ^{1}H 64-step small-phase incremental alternation (SPINAL-64) decoupling[52] was applied during the signal acquisition. Typically 4096 transients were accumulated for each sample with 2 s recycle delay.

The ^{29}Si NMR spectra were recorded either using a single pulse experiment (5 μs 90° pulse length, 10 s recycle delay, about 6000 transients per sample) or a ^{1}H→^{29}Si CPMAS sequence (7.5 ms contact time, 2 s relaxation time, about 6000 transients per sample). Deconvolution of the single-pulse ^{29}Si MAS NMR spectrum of HB provides the Si/Al ratio[50] (Table 2). The ^{1}H-^{29}Si CP heteronuclear (CP-HETCOR) NMR spectra of samples SD/AgB and AgSD/HB were recorded using similar CP conditions, 40 t_1 slices with 1024 transients each.

Table 2. Composition and structure characteristics of the parent (HB) and Ag modified (AgB) BEA materials.

Sample	Bulk Si/Al (molar ratio)[a]	Framework Al (%)[b]	Extra framework Al (%)[b]	BET (m^2/g)[c]	External surface area (m^2/g)[c]	V_{total} (cm^3/g)[c]	V_{Micro} (cm^3/g)[c]	V_{Meso} (cm^3/g)[c]
HB	8	78	22	761	345	0.462	0.119	0.343
AgB	8	100	0	341	138	0.212	0.089	0.123

[a]The molar framework Si/Al ratio was determined on the basis of the NMR data.[50]
[b]According to deconvoluted ^{27}Al NMR spectrum of the parent HB zeolite (Figure S1, ESI).
[c]Determined in [51].

Quantitative ^{27}Al MAS NMR spectra were recorded using a single pulse experiment (1 μs pulse length, corresponding to a flip angle below 30°). Typically 6000 transients were accumulated for each sample with 0.5 s recycle delay. Deconvolution of the ^{27}Al NMR spectrum of HB provides the relative concentration of lattice and extra-lattice Al atoms (Table 2 and Figure S1, ESI).

The ^{1}H T_1 (inversion-recovery) and T_2 (Hahn-echo) measurements were performed on the pure drugs and on the loaded zeolites, previously dried at 100 °C overnight. The MAS frequency was 20 kHz. The T_2 curves were fitted with a single exponential decay for the pure drugs while two-exponential fit was needed for the drugs loaded in the zeolites.

The ^{1}H, ^{13}C and ^{29}Si chemical shifts were externally referenced to proton, carbon and silicon signals in TMS. The ^{27}Al chemical shifts were references to a 1M solution of $Al(NO_3)_3$. The NMR spectra were analyzed using the Dmfit software.[53]

N_2 adsorption experiments were performed with a Micromeritics ASAP 2010 surface area analyzer. The samples were outgassed at 300°C prior the measurement. The specific surface (BET) area, the total pore volume, V_{total} (determined from the N_2 uptake at P/P_0 = 0.95), the micropore volume, V_{micro}, and external surface area (according to **n***(C*BET*)* plots [54,55]), the mesopore volume, V_{meso} (as difference between V_{tot} and V_{MI}), were calculated (Table 2) on the basis of the N_2 adsorption–desorption isotherms.

Conclusions

Solid state NMR was applied for detailed characterization of zeolite Beta-based dual drug formulations with antibacterial properties, containing Ag and SD. The ^{27}Al NMR spectra showed that the loading of SD, Ag or AgSD resulted in a reinsertion of the EFAl into the zeolite matrix of the HB parent carrier. The mechanism of EFAl inclusion involves exchange between the zeolite protons and H^+ or Ag^+ cations, originating from SD and AgSD respectively, that play a role of charge compensating species. The loaded drug (SD, AgSD) is predominantly localized in the vicinity of Si(0Al) groups and a larger amount of it is most probably embedded within the zeolite pores. The amount of the SD drug confined into the pores of HB zeolite is higher than that included into the Ag modified carrier. ^{1}H-^{29}Si HETCOR spectra of SD/AgB and AgSD/HB samples show similar correlation patterns, which is an evidence for the analogous localization of the drug into the zeolites. The ^{1}H spin-lattice and spin-spin relaxation times indicate that the drug molecules incorporated into the zeolite matrix by the applied preparation procedure are in amorphous form.

Acknowledgements

The authors are grateful to Dr. V. Valtchev from Laboratoire Catalyse & Spectrochimie, ENSICAEN, Université de Caen, France, for providing the parent freeze-dried zeolite Beta.

Notes and references

1 M. Rai, K. Kon, A. Ingle, N. Duran, S. Galdiero, M. Galdiero, *Appl. Microbiol. Biotechnol.* 2014, **98**, 1951.
2 N.H. Chau, L.A. Bang, N.Q. Buu, T.T.N. Dung, H.T. Ha, D.V. Quang, *Adv. Nat. Sci.* 2008, **9**, 241.
3 T.T.N. Dung, N.Q. Buu, D.V. Quang, H.T. Ha, L.A. Bang, N.H. Chau, N.T. Ly, N.V. Trung, *J. Phys. Conf. Ser.* 2009, **187**, 012054.
4 M. Zaarour, B. Dong, I. Naydenova, R. Retoux, S. Mintova, *Micropor. Mesopor. Mater.* 2014, **189**, 11.
5 M. Rai, A. Yadav, A. Gade, *Biotechn. Adv.* 2009, **27**, 76.
6 P. Laluesa, M. Monzon, M. Arruebo, J. Santamaria, *Chem. Commun.* 2011, **47**, 680.
7 P. Laluesa, D. Carmona, M. Monzon, M. Arruebo, J. Santamaria, *Micropor. Mesopor. Mater.* 2012, **156**, 171.
8 K. Pavelic, B. Subotic, M. Colic, in: A. Galarneau, F. Di Renzo, F. Fajula, J. Vedrine (Eds.), Zeolites and Mesoporous Materials at the Dawn of the 21st Century, *Stud. Surf. Sci. Catal.*, vol. 135, Elsevier, Amsterdam, 2001, p. 32-O-01.
9 A. Dyer, S. Morgan, P. Wells, C. Williams, *J. Helminthol.* 2000, **74**, 137.
10 S. Grund, T. Doussineau, D. Fisher, G. Mohr, *J. Coll. Interf. Sci.* 2012, **365**, 33.
11 R. Amorin, N. Vilaca, O. Martinho, R.M. Reis, M. Sardo, J. Rocha, A. M. Fonseca, F. Baltazar, I. C. Neves, *J. Phys. Chem. C* 2012, **116**, 25642.
12 E. Khodaverdi, R. Honarmandi, M. Alibolandi, R. Rafatpanah Baygi, F. Hadizadeh, G.Zohuri, *Iran J. Basic Med. Sci.* 2014, **17**, 337**.**
13 I. Braschi, G. Gatti, G. Paul, C.E. Gessa, M.Cossi, L. Marchese, *Langmuir* 2010, **26**, 9524.
14 I. Braschi, S. Blasioli, L.Gigli, C.E. Gessa, A. Alberti, A. Martucci, *J. Hazard. Mater.* 2010, **178**, 218.
15 I. Braschi, G. Paul. G. Gatti, M. Cossi, L. Marchese, *RSC Adv.* 2013, **3**, 7427.
16 A. Rivera, M.L. Rodrıguez-Albelo, G. Rodrıguez-Fuentes, E. Altshuler, in: A. Galarneau, F. Di Renzo, F. Fajula, J. Vedrine (Eds.), Zeolites and Mesoporous Materials at the Dawn of the 21st Century, *Stud. Surf. Sci. Catal.*, vol. 135, Elsevier, Amsterdam 2001, p. 32-P-07.
17 P. Horcajada, C. Marquez-Alvarez, A. Ramila, J. Perez-Pariente, M. Vallet-Regi, *Solid State Sci.* 2006, **8**, 1459.
18 A. Datt, E.A. Burns, N. A. Dhuna, S.C. Larsen, *Micropor. Mesopor. Mater.* 2013, **167**, 182.
19 A. Datt, D. Fields, S.C. Larsen, *J. Phys. Chem. C* 2012, **116**, 21382.
20 S. Mintova, M. Jaberboc, V. Valtchev, *Chem. Soc. Rev. 2015*, From themed collection Recent Advances in Zeolite Chemistry and Catalysis, Nanosized microporous crystals: emerging applications.
21 D. Fatouros, D. Douroumis, V. Nicolakis, S. Ntais, A. Moschovi, V. Trivedi, B. Khima, M. Roldo, H. Nazar, P.A. Cox, *J. Mater. Chem.* 2011, **21**, 7789.
22 Y. Matsumura, K. Yoshikata, S. Kunisaki, T. Tsuchido, *Appl. Environ Microbiol.* 2003, **69**, 4278.
23 T. Kihara, Y. Zhang, Y. Hu, Q. Mao, Y. Tang, J. Miyake, *J. Biosci. Bioeng.* 2011, **111**, 725.

24 M. Potara, E. Jakab, A. Damert, O. Popescu, V. Canpean, S. Astilean, *Nanotechnology* 2011, **22**, 35101.
25 P. Li, J. Li, C. Wu, Q. Wu, J. Li, *Nanotechnology* 2005, **16**, 1912.
26 G. Cerri, M. de'Gennaro, M.C. Bonferoni, C. Caramella, *Appl. Clay Sci.* 2004, **27**, 141.
27 R. M. E. Richards, R. B. Taylor, D. K. L. Xing, *J. Pharm. Sci.* 1991, **80**, 861.
28 R. M. E. Richards, D. K. L. Xing, *Int. J. Pharm.* 1991, **75**, 81.
29 V. Mavrodinova, M. Popova, K. Yoncheva, J. Mihály, A. Szegedi, *J. Coll. Interf. Sci.* 2015, **458**, 32.
30 T. Azais, C. Tourne-Peteilh, F. Aussenac, N. Baccile, C. Coelho, J.-M. Devoisselle, F. Babonneau, *Chem. Mater.* 2006, **18**, 6382.
31 J. Trebosc, J. W. Wiench, S. Huh, V. S. Y. Lin, M. Pruski, *J. Am. Chem. Soc.* 2005, **127**, 3057.
32 E. Skorupska, A. Jeziorna, S. Kazmierski, M.J. Potrzebowski, *Solid State Nucl. Magn. Reson.* 2014, **57-58**, 2.
33 M. Fatnassi, C. Tourne-Peteilh, T. Mineva, J-M. Devoisselle, P. Geveau, F. Fayon, B. Alonso, *Phys. Chem. Chem. Phys.* 2012, **14**, 12285.
34 T. Ukmar, T. Cendak, M. Mazaj, V. Kaucic, G. Mali, *J. Phys. Chem. C* 2012, **116**, 2662.
35 G. Engelhardt, U. Lohse, S. Samoson, M. Maegi, M. Tarmak, E. Lippmaa, *Zeolites* 1982, **2**, 59.
36 E. Bourgeat-Lami, P. Massiani, F. Di Renzo, P. Espiau, F. Fajula, *Applied Catalysis* 1991, **72**, 139.
37 G. H. Kuehl, H. K. C. Timken, *Micropor. Mesopor. Mater.* 2000, **35-36**, 521.
38 S. Altwasser, J. Jiao, S. Steuernagel, J. Weitkamp, M. Hunger, in: E. van Santen, L. Callanan, M. Claeys (Eds.), *Studies in Surface Science and Catalysis*, Elsevier 2004, v. 154, 3098.
39 C. Jia, P. Massiani, D. Barthomeuf, *J. Chem. Soc., Faraday Trans.* 1993, **89**, 3659.
40 J. A. van Bokhoven, A. M. J van der Eerden, D. C. Koningsberger, *J. Am. Chem. Soc.* 2003, **125**, 7435.
41 D. Ma, F. Deng, R. Fu, X. Han, X. Bao, *J. Phys. Chem. B* 2001, **105**, 1770.
42 D. Freude, H. Ernst, I. Wolf, *Solid State Nucl. Magn. Reson.* 1994, **3**, 271.
43 B. H. Wouters, T.-H. Chen, P. J. Grobet, *J. Am. Chem. Soc.* 1998, **120**, 11419.
44 E. van Eck, J. Pieterse, A. Kentgens, Solid State Nucl. Magn. Reson. 2011, **39**, 99.
45 Z. Yu, A. Zheng, Q. Wang, L. Chen, Jun Xu, J.-P. Amoureux, F. Deng, *Angew. Chem. Int. Ed.* 2010, **49**, 8657.
46 P. J. Kunkeler, B. J. Zuurdeeg, J. C. van der Waal, J. A. van Bokhoven, D. C. Koningsberger, H. van Bekkum, *J. Catal.* 1998, **180**, 234.
47 L. Ding, Y. Zheng, Y. Hong, Z. Ring, *Micropor. Mesopor. Mater.* 2007, **101**, 432.
48 T.-H. Chen, K. Houthoofd, P. J. Grobet, *Micropor. Mesopor. Mater.* 2005, **86**, 31.
49 M. L. Landau, D. Tavor, O. Regev, M. L. Kalija, M. Herskowitz, V. Valtchev, S. Mintova, *Chem. Mater.* 1999, **11**, 2030.
50 J. Klinowski, S. Ramdas, J. M. Thomas, C. A. Fyfe, J. S. Hartman, *J. Chem. Soc., Faraday Trans. II* 1982, **78**, 1025.
51 V. Mavrodinova, M. Popova, V. Valchev, R. Nickolov, Ch. Minchev, *J. Coll. Interf. Sci.* 2005, **286**, 268.
52 B. M. Fung, A. K. Khitrin, K. Ermolaev, *J. Magn. Reson.* 2000, **142**, 97.
53 D. Massiot, F. Fayon, M. Capron, I. King, S. Le Calvé, B. Alonso, J. O. Durand, B. Bujoli, Z. Gan, G. Hoatson, *Magn. Reson. Chem.* 2002, **40**, 70.
54 A. J. Lecloux, in: J. Anderson, M. Bondartm (Eds.), Catalysis: Science and Technology, vol. 2, Springer-Verlag, New York 1981, p. 171.
55 A. J. Lecloux, J. Pirard, *J. Colloid Interface Sci.* 1979, **70**, 265.

Table of Contents

Solid state NMR characterization of zeolite Beta based drug formulations containing Ag and sulfadiazine

Pavletta Shestakova,*[a] Charlotte Martineau,[b] Vesselina Mavrodinova[a] and Margarita Popova[a]

The paper presents an investigation of structural changes of zeolite carrier, drug-matrix interactions and localization of dru molecules within the zeolite framework in dual drug formulations with antibacterial properties.